ISSN (Print) 1226-1750
ISSN (Online) 2233-6656
Journal of Magnetics 18(2), 117-124 (2013) http://dx.doi.org/10.4283/JMAG.2013.18.2.117

A Novel Cogging Torque Reduction Method for Single-Phase Brushless DC Motor

Young-Un Park[1], Ju-Hee Cho[2], Se-Hyun Rhyu[3], and Dae-Kyong Kim[1]*

[1]*Department of Electrical Control Engineering, Sunchon National University, Suncheon 540-950, Korea*
[2]*Korean Electronics Technology Institute (KETI), Gwangju 500-480, Korea*
[3]*Korean Electronics Technology Institute (KETI), Buchon 203-103, Korea*

(Received 27 January 2013, Received in final form 13 April 2013, Accepted 30 April 2013)

Single-phase, brushless DC (BLDC) motors have unequal air-gaps to eliminate the dead-point where the developed torque is zero. Unfortunately, these unequal air-gaps can deteriorate the motor characteristics in the cogging torque. This paper proposes a novel design for a single-phase BLDC motor with an asymmetric notch to solve this problem. In the design method, the asymmetric notches were placed on the stator pole face, which affects the change in permanent magnet shape or the residual flux density of the permanent magnet. Parametric analysis was performed to determine the optimal size and position of the asymmetric notch to reduce the cogging torque. Finite element analysis (FEA) was used to calculate the cogging torque. A more than 28% lower cogging torque compared to the initial model with no notch was achieved.

Keywords : asymmetric air-gap, asymmetric position notch, cogging torque, single phase brushless DC motor

1. Introduction

Single-phase brushless DC (BLDC) motors are used widely in blowers for ventilation systems and home appliances because of their high efficiency and cost effectiveness. Single-phase BLDC motors with a uniform air-gap make them inherently non-self starting because of their coincident zero torque positions of excitation. Therefore, single-phase BLDC motors adopt asymmetric air-gaps to make them self starting [1-3]. On the other hand, such an asymmetric air-gap can contribute to cogging torque [4-6].

The conventional methods for reducing the cogging torque of single-phase BLDC motors include the length change of the air-gap, PM asymmetry arrangement, skew of the stator or rotor and shape change of the stator teeth. Some papers reported reductions in the cogging torque for single-phase BLDC motors by varying the air-gap profile, considering the tapered teeth and the trailing edge of teeth [7, 8].

Some approaches have proposed the analytical model capable of predicting the cogging torque [9-11] and changing the design parameter such as teeth notching [12, 13] for symmetric air-gap. The analytical methods are effective to find the parameters quickly for reducing cogging torque. However, the analytical methods are not suitable to accurately predict the cogging torque for such single-phase BLDC motors with asymmetric air-gaps.

This paper reports a novel cogging torque reduction method that applies size and asymmetric position variations of the notches to the tapered teeth of a stator in a single-phase BLDC motor for a fan of ventilation system, as shown in Fig. 1. Finite-element analysis (FEA) was used to calculate the cogging torque. Parametric analysis using FEA was performed to determine the optimal size and position of the asymmetric notches to reduce the cogging torque. This proposed stator shape with an asymmetric position notch was compared with the initial model, and the measured performance of the cogging torque was analyzed.

2. Analytical Expression for Cogging Torque

The cogging torque is the amount of energy variation according to the amount of rotor rotation and can be expressed as Eq. (1) [9-13].

$$T_{cog} = -\frac{\Delta W(\alpha)}{\Delta \alpha} \tag{1}$$

*Corresponding author: Tel: +82-61-750-3546
Fax: +82-61-753-3546, e-mail: dkkim@sunchon.ac.kr

where W is the magnetic energy of the machine and α is the position angle of the rotor.

For the surface permanent magnet type of BLDC, most of the energy change occurs on the air-gap part. Therefore, only the energy on the air-gap part is considered when calculating the cogging torque. The air-gap energy is calculated from the air-gap magnetomotive force function, $F(\theta, \alpha)$, and air-gap permeance function $P(\theta)$ according to Eq. (2)

$$W(\alpha) = \frac{1}{2\mu_0}\int_V \{F(\theta, \alpha)\cdot P(\theta)\}^2 dV \tag{2}$$

where the air-gap magnetomotive force function and the air-gap permeance function can be expressed as follows:

$$F(\theta) = \frac{g}{2\mu_0}B(\theta) \tag{3}$$

$$P(\theta) = \frac{\mu_0}{g}G(\theta) \tag{4}$$

where g is the air-gap length.

The air-gap energy can be calculated again as follows:

$$\begin{aligned} W(\alpha) &= \frac{1}{2\mu_0}\int_V \{F(\theta, \alpha)\cdot P(\theta)\}^2 dV \\ &= \frac{1}{2\mu_0}\int_V \{B(\theta, \alpha)\cdot G(\theta)\}^2 dV \\ &= \frac{1}{2\mu_0}\int_0^{L_s}\int_{R_s}^{R_m}\int_0^{2\pi} \{B(\theta, \alpha)\cdot G(\theta)\}^2 d\theta r\, dr\, dz \\ &= \frac{L_s}{4\mu_0}(R_m^2 - R_s^2)\int_0^{2\pi} B(\theta, \alpha)^2\cdot G(\theta)^2 d\theta \end{aligned} \tag{5}$$

where B, G, R_m and R_s are the flux density, relative air-gap permeance function, inner radius of the rotor and inner radius of the stator, respectively.

$B(\theta, \alpha)^2$ and $G(\theta)^2$ can be calculated through a Fourier series expansion used in Eq. (5) on an even function as follows:

$$B(\theta, \alpha)^2 = \sum_{n=0}^{\infty} B_{n N_s}\cos(n N_p(\theta+\alpha)) \tag{6}$$

$$G(\theta)^2 = \sum_{n=0}^{\infty} G_{n N_s}\cos(n N_s\theta) \tag{7}$$

where N_p is the number of rotor poles and N_s the number of stator slots.

The air-gap energy obtained by substituting Eqs. (6) and (7) for Eq. (5) can be represented as Eq. (8), as follows:

$$\begin{aligned} W(\alpha) &= \frac{L_s}{4\mu_0}(R_m^2 - R_s^2) \\ &\quad \left\{\int_0^{2\pi}\sum_{n=0}^{\infty} B_{n N_L}G_{n N_s}\cos(n N_L(\theta+\alpha))\cos(n N_L\theta)d\theta\right\} \\ &= \frac{L_s}{4\mu_0}(R_m^2 - R_s^2)\sum_{n=0}^{\infty} B_{n N_L}G_{n N_s}\cos(n N_L\alpha) \end{aligned} \tag{8}$$

where L_s is the stack height and N_L is the least common multiple of N_p and N_s.

The final cogging torque can be represented as Eq. (9) by differentiating the air-gap energy obtained from Eq. (8) according to Eq. (1) with a rotation angle of the rotor [10, 11].

$$T(\alpha) = \frac{L_s\pi}{4\mu_0}(R_m^2 - R_s^2)\sum_{n=0}^{\infty} B_{n N_L}G_{n N_L} n N_L\sin(n N_L\alpha) \tag{9}$$

According to Eq. (9), the cogging torque is determined from the values of B_{nN_L} and G_{nN_L}. Here, when a notch is applied to the stator teeth, the shape of the relative air-gap function begins to change, and the N_L value changes with the number of valid slots (sum of numbers of actual slots and notches). In addition, the notch can use more than two notches if the stator shoe width has a sufficient gap.

If the permeance function of the air-gap assumes that the part that applied the notch qual to 0, it can gain the

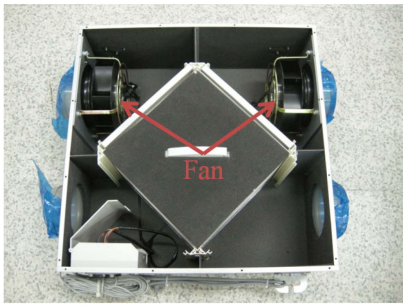

(a)

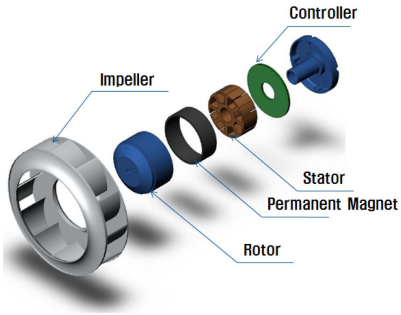

(b)

Fig. 1. (Color online) Configuration of the ventilation system (a) Prototyped ventilation system (b) Components of single-phase BLDC motor.

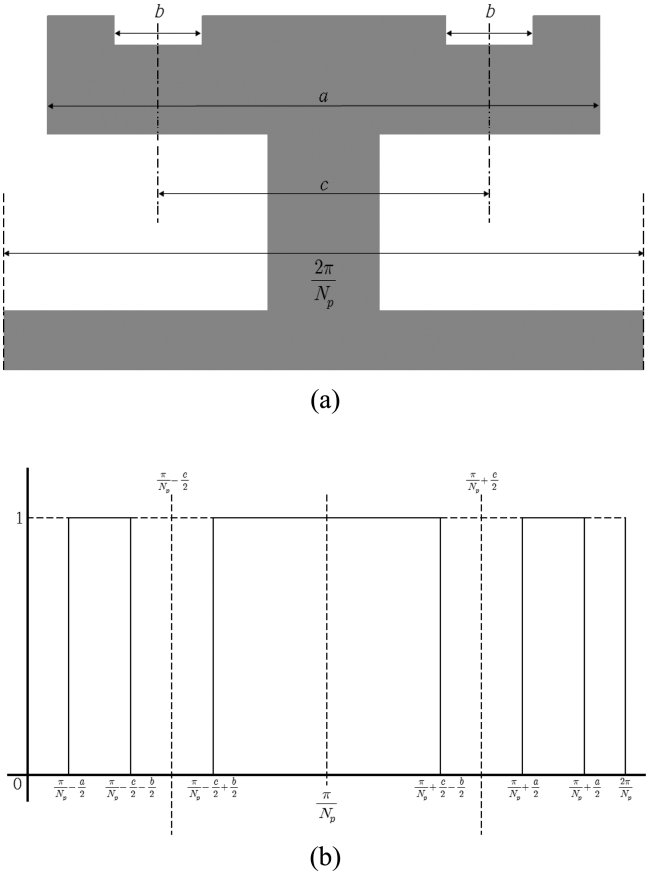

Fig. 2. Stator shape applied two notches (a) Stator shape (b) Relative permeance function.

shape shown in Fig. 2, which can be represented as Eq. (10) through a Fourier series expansion of the relative permeance function. If the stator teeth design such that the harmonics term of the air-gap permeance, Fourier coefficient changes and the harmonics term increases due to the influence of the notch, the frequency of harmonics increases and the size decreases eventually resulting in a decrease in cogging torque. Therefore, if teeth size is constant, notch size and notch position can be as dominant parameters for reducing cogging torque as Eq. (10) [9].

$$G_{n\,N_L}=\frac{N_s}{\pi}\left\{\int_{\frac{\pi}{N_p}-\frac{a}{2}}^{\frac{\pi}{N_p}-\frac{c}{2}-\frac{b}{2}}\cos nN_L\theta d\theta+\int_{\frac{\pi}{N_p}-\frac{c}{2}+\frac{b}{2}}^{\frac{\pi}{N_p}+\frac{c}{2}-\frac{b}{2}}\cos nN_L\theta d\theta+\int_{\frac{\pi}{N_p}+\frac{c}{2}+\frac{b}{2}}^{\frac{\pi}{N_p}+\frac{a}{2}}\cos nN_L\theta d\theta\right\}$$

$$=\frac{N_s}{\pi\, n\, N_L}[\sin nN_L\theta]_{\frac{\pi}{N_p}-\frac{a}{2}}^{\frac{\pi}{N_p}-\frac{c}{2}-\frac{b}{2}}+[\sin nN_L\theta]_{\frac{\pi}{N_p}-\frac{c}{2}+\frac{b}{2}}^{\frac{\pi}{N_p}+\frac{c}{2}-\frac{b}{2}}+[\sin nN_L\theta]_{\frac{\pi}{N_p}+\frac{c}{2}+\frac{b}{2}}^{\frac{\pi}{N_p}+\frac{a}{2}}$$

$$=\frac{2N_s}{\pi\, n\, N_L}\left[(-1)^{\frac{nN_L}{N_p}}\left\{\sin nN_L\left(\frac{a}{2}\right)-\sin nN_L\left(\frac{b+c}{2}\right)+\sin nN_L\left(\frac{-b+c}{2}\right)\right\}\right] \quad (10)$$

where, a is teeth size, b is notch size and c is notch position.

3. Novel Cogging Torque Reduction Method

3.1. Conventional stator structure of single-phase BLDC motor

A general single-phase BLDC motor can cause the failure of a trial run because its rotor is arranged where torque is not generated. Therefore, the rotor needs to be arranged where the torque can be generated by the asymmetric shape of the stator.

3.2. Concept of Cogging Torque Reduction Method for single-phase BLDC Motor

BLDC motors with a permanent-magnet inevitably show a cogging torque because of the changes caused by the permanent-magnet of the rotor and the magnetic force of the stator core. Eq. (1) shows the cogging torque. From Eq. (1), the rate of change in the magnetic force should be minimized to reduce the cogging torque as much as possible. The magnetic energy is determined by B and G, as expressed in Eq. (5). In the case of a single-phase BLDC motor with an asymmetric air-gap as shown in Fig. 3(a), B and G are asymmetric according to the rotation of the rotor.

In case of adopting notch for tapered-teeth, the application of an asymmetric notch position and size to the teeth is required as the dominant parameters as like Eq. (10) for reducing cogging torque for the single-phase BLDC motor.

FEA is suitable to accurately predict the cogging torque of the single-phase BLDC motor with an asymmetric air-gap. Parametric analysis using FEA was performed to determine the optimal size and position of the asymmetric notches to reduce the cogging torque. Therefore, the size and position of the asymmetric notch applied to tapered-teeth are proposed, as shown in Fig. 3(b).

3.3. Parametric analysis of the cogging torque using FEA

This paper presents the 120[W] class single-phase BLDC with an 8 pole/8 slot structure. Table 1 lists the specifications of the proposed single-phase BLDC motor. Fig. 4 shows the size and position angle variation of the notch.

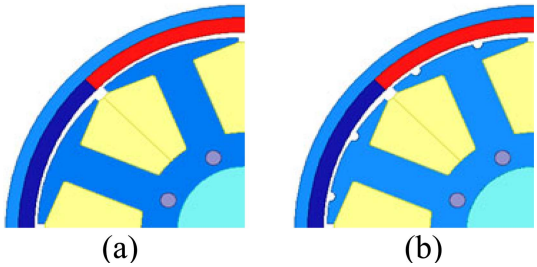

Fig. 3. (Color online) Single-phase BLDC motor structure (a) Initial model (tapered-teeth) (b) Proposed model.

Table 1. Specifications of the Single-Phase BLDC Motor.

Parameter	Unit	Value
Rated Output	W	123
Rated Torque	Nm	0.382
Rated Speed	rpm	3,000
Input Voltage	V_{ac}	220
Outer diameter	mm	92
Average radial air-gap length	mm	0.5
Stack length	mm	30
Magnet thickness	mm	3

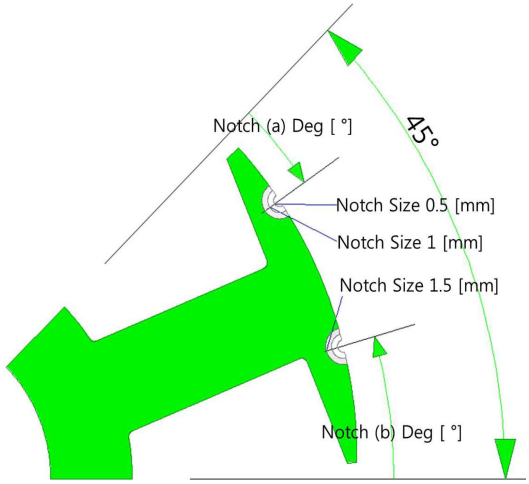

Fig. 4. (Color online) Size and position angle variation of the notch.

We are adopted two notches because it is easy to predict trends of cogging torque variation according to different position angle and size of the notch. Parametric analysis was performed to determine the optimal size and position of the asymmetric notch to reduce the cogging torque using FEA. Figs. 5, 6 and 7 show the results of parametric analysis of the cogging torque according to the position angle of the notch (b) variation at 0.5[mm], 1.0[mm], and 1.5[mm], respectively. The cogging torque was at lowest (43.6[mNm]) when the position angle of notch(a) and notch(b) were 10° and 15°, respectively, at a 1.0[mm] notch size.

Fig. 8 shows the cogging torque from the initial and proposed model. The peak to peak cogging torque of the initial and proposed model were 60.27[mNm] and 43.25 [mNm], respectively. The cogging torque reduction ratio of the proposed model was approximately 28.2% compared to the initial model from FEA. Fig. 9 shows the magnetic flux distributions of the initial and proposed model.

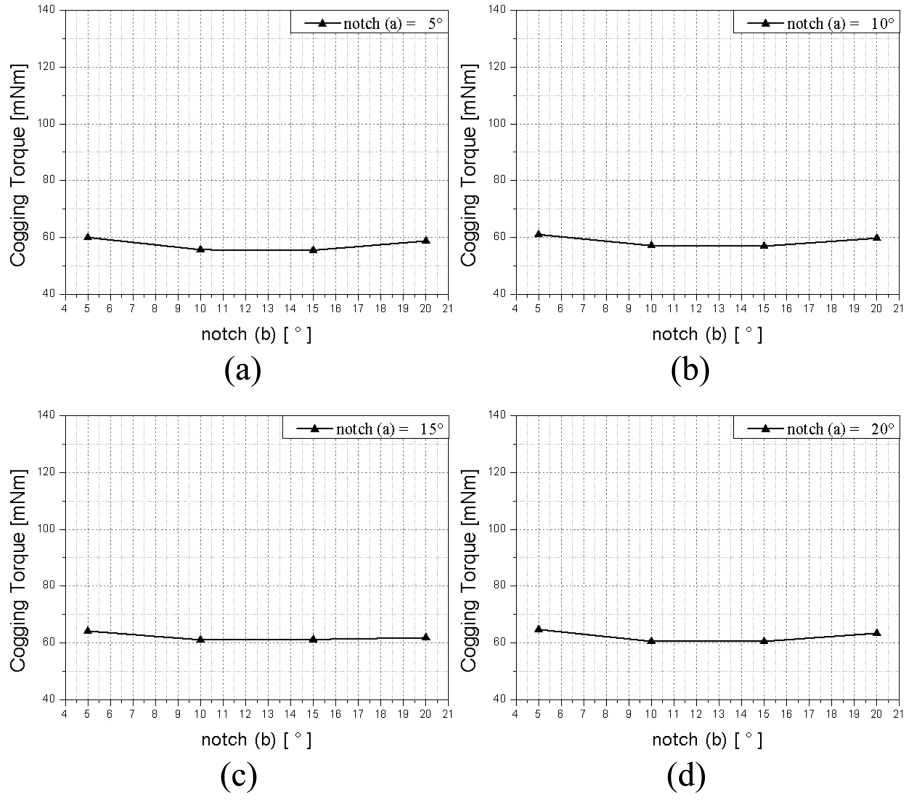

Fig. 5. Parametric analysis results of the cogging torque according to the position angle of notch (b) variation at 0.5[mm] notch size (a) notch (a) = 5°, (b) notch (a) = 10°, (c) notch (a) = 15°, (d) notch (a) = 20°.

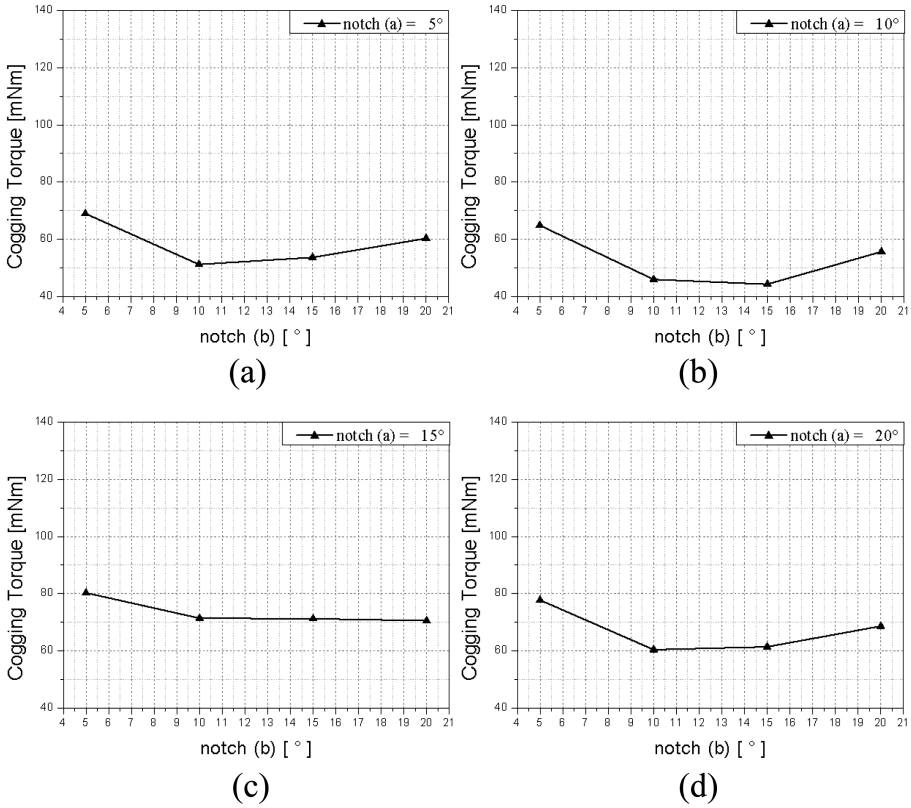

Fig. 6. Parametric analysis results of the cogging torque according to the position angle of the notch (b) variation at 1.0[mm] notch size (a) notch (a) = 5°, (b) notch (a) = 10°, (c) notch (a) = 15°, (d) notch (a) = 20°.

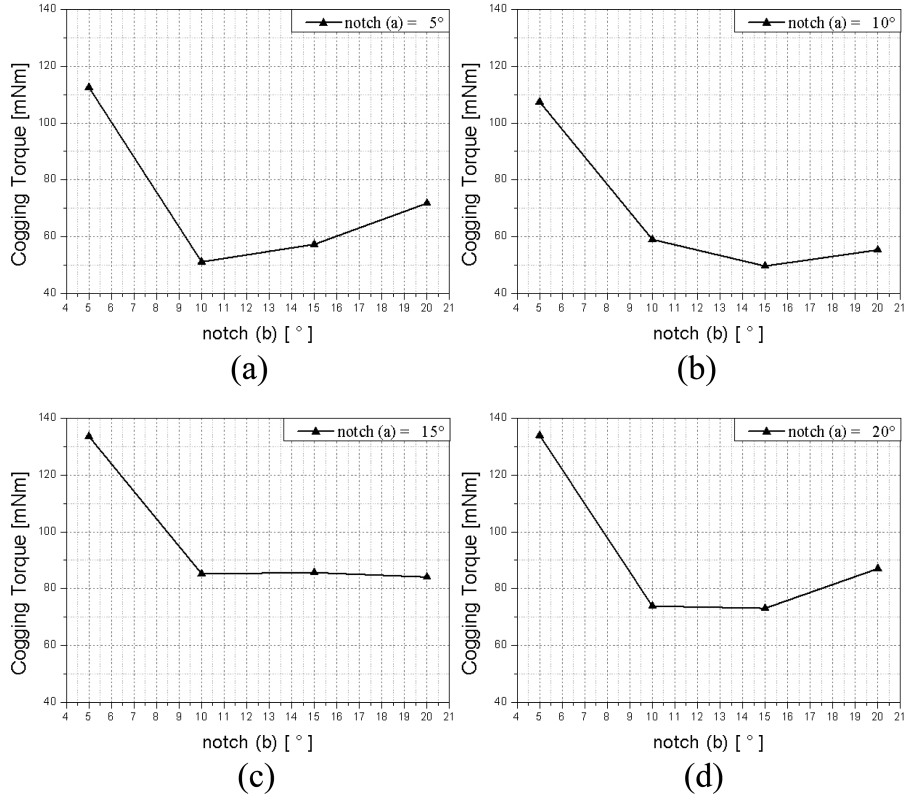

Fig. 7. Parametric analysis results of the cogging torque according to the position angle of the notch (b) variation at 1.5[mm] notch size (a) notch (a) = 5°, (b) notch (a) = 10°, (c) notch (a) = 15°, (d) notch (a) = 20°.

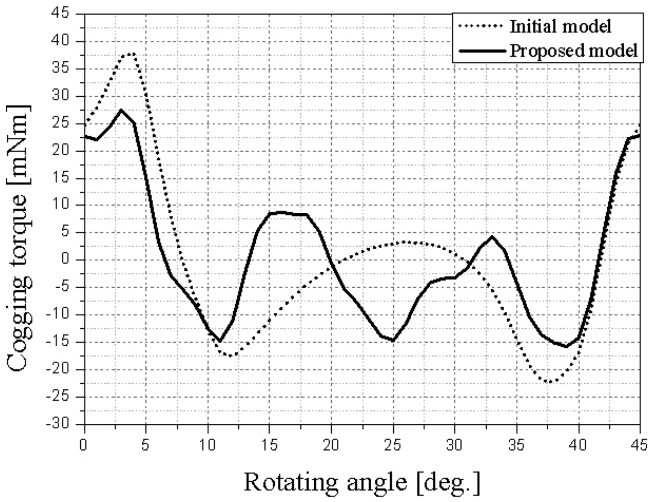

Fig. 8. Analysis results of the cogging torque of the initial and proposed model.

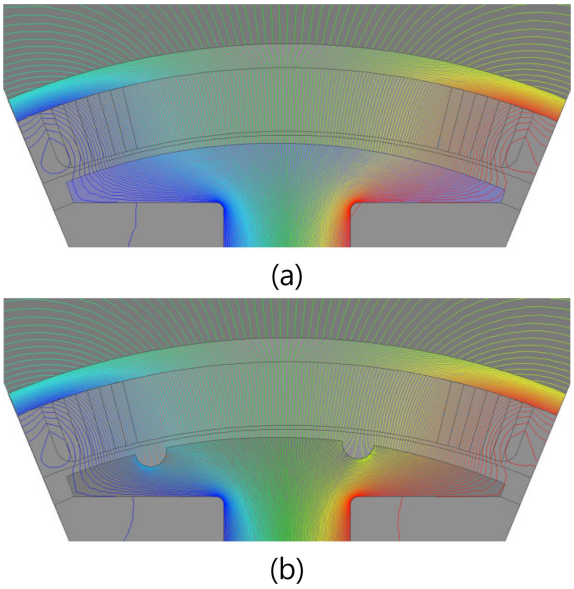

Fig. 9. (Color online) Flux distributions (a) initial model (b) proposed model.

4. Experimental Results

Fig. 10 presents the manufactured stators of the initial and proposed model and rotor for the experiment. The properties of the proposed cogging torque reduction method were verified experimentally. Fig. 11 shows the test equipment used to measure the cogging torque. The cogging torque meter with a 0.001% RPM accuracy was made by SUGAWARA in Japan.

Fig. 12 compares the experimentally determined cogging torque of the initial and proposed model. The peak to peak cogging torque of the initial and proposed model

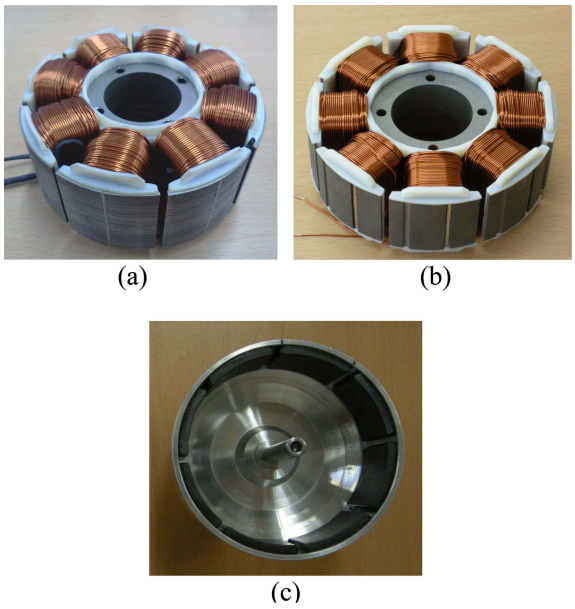

Fig. 10. (Color online) Manufactured single-phase BLDC motor (a) initial model (b) proposed model (c) rotor.

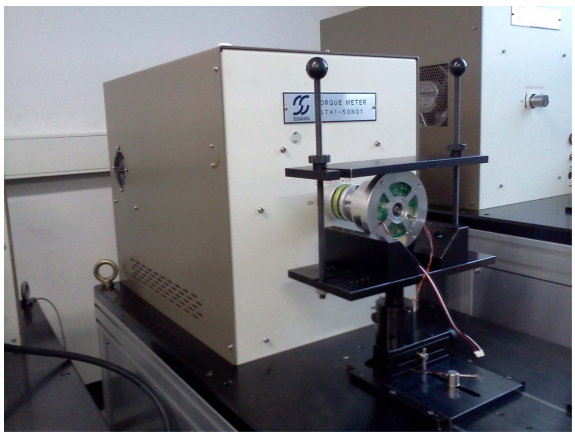

Fig. 11. (Color online) Test equipment for measuring the cogging torque.

were 65.94[mNm] and 46.88[mNm], respectively. The cogging torque reduction ratio of the proposed model was approximately 28.9% compared to the initial model. The period and magnitude of the cogging torque were similar to the results of FEA.

A sound quality experiment under the ventilation system was also performed for the initial and proposed model. Fig. 13 shows the experimental sets for the sound noise measurement under anechoic room (19[dB] background noises). Fig. 14 shows the experimental results of the average sound noise test for the ventilation system for 100[sec]. The average sound noise of the initial and proposed model was 55[dB] and 49.6[dB], respectively, indicat-

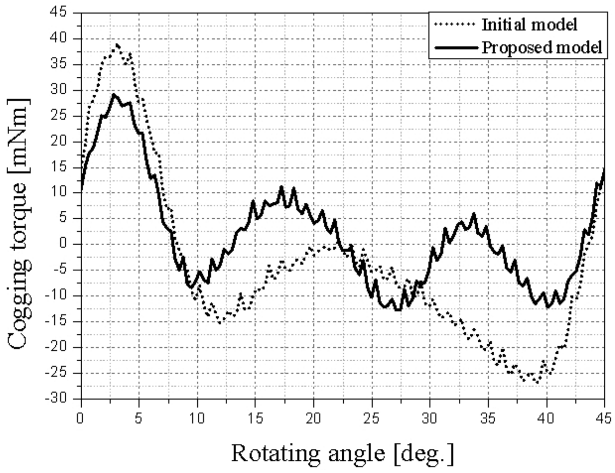

Fig. 12. Experimental results of the cogging torque of the initial and proposed model.

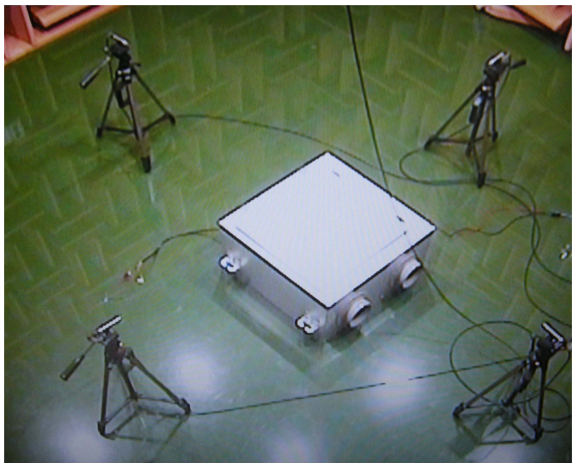

Fig. 13. (Color online) Equipment for sound quality test.

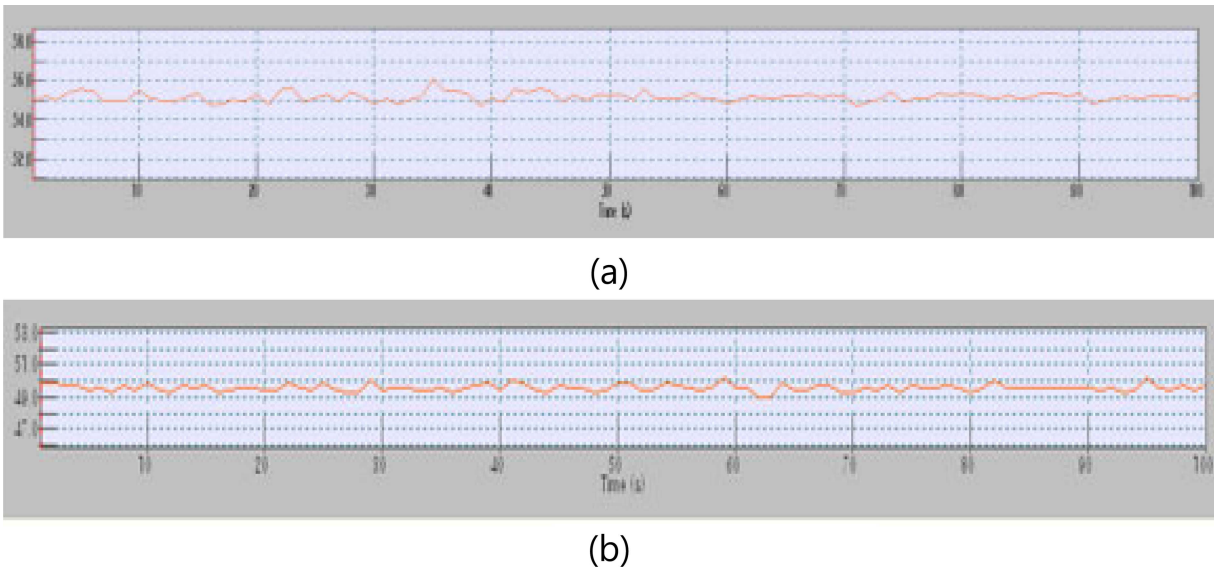

Fig. 14. (Color online) Experimental results of the average sound test for ventilation system during 100[sec] (a) Initial model (55 [dB]) (b) Proposed model (49.6 [dB]).

ing the proposed model to produce an approximately 10% reduction in noise.

5. Conclusion

This paper examined the stator shape of a motor stator and developed a method to reduce the cogging torque. This method produced a 28% and 10% decrease in cogging torque and sound noise, respectively, compared to that obtained using the initial model. The experimental results of the cogging torque confirmed the FEA results. This method is considered to be a good alternative for reducing the cogging torque of single-phase brushless motors.

Acknowledgment

This work was supported by the New & Renewable Energy of the Korea Institute of Energy Technology Evaluation and Planning (KETEP) grant funded by the Korea government Ministry of Knowledge Economy (No. 20113030060010).

References

[1] Y. Chen, S. Chen, Z. Q. Zhu, D. Howe, and Y. Y. Ye, IEEE Trans. Magn. **42**, 3416 (2006).
[2] Chun-Lung Chiu, Yie-Tome Chen, and Wun-Siang Jhang,

IEEE Trans. Magn. **44**, 2317 (2008).
[3] Mohammed Fazil and K. R. Rajagopal. IEEE Trans. Magn. **46**, 3928 (2010).
[4] A. Hamler and B. Hribernik, IEEE Trans. Magn. **32**, 1545 (1996).
[5] D. R. Huang, T. F. Ying, C. M. Zhou, Y. K. Lin, K. W. Su, and C. I. Hsu, IEEE Trans. Magn. **34**, 2075 (1998).
[6] K. Bung-Il, Byoung-Yull Yang, Y. Byoung-Yull, P. Seung-Chan, and J. Young-Sun, IEEE Trans. Magn. **37**, 3723 (2001).
[7] Weizi Wang, Zhigan Wu, Wanbing Jin, and Jianping Ying, IEEE Conference IECON, 1605 (2005).
[8] S. Ahmed and P. Lefley, International conference EPECS 1 (2009).
[9] J. De La Ree and N. Boules, IEEE Trans. Industry Appl. **25**, 107 (1989).
[10] Li Zhu, S. Z. Jiang, and Z. Q. Zhu, IEEE Trans. Magn. **45**, 2023 (2009).
[11] Daohan Wang, Xiuhe Wang, Dongwei Qiao, Ying Pei, and Sang-Yong Jung, IEEE Trans. Magn. **47**, 2231 (2011).
[12] Yubo Yang, Xiuhe Wang, Changqing Zhu, and Chuanzhen Huang, IEEE Conference ICIEA 2325 (2009).
[13] Bin Zhang, Xiuhe Wang, Ran Zhang, and Xiaolei Mou, ICEMS Conference 3198 (2008).